ARTICLE

OBC
www.rsc.org/obc

# The reaction of *S*-nitroso-*N*-acetyl-D,L-penicillamine (SNAP) with the angiotensin converting enzyme inhibitor, captopril—mechanism of transnitrosation†

**Danielle V. Aquart and Tara P. Dasgupta***

*Department of Chemistry, University of the West Indies, Mona Campus, Kingston 7, Jamaica. E-mail: tara.dasgupta@uwimona.edu.jm; Fax: 876-977-1835*

***Received 20th January 2005, Accepted 14th March 2005***
***First published as an Advance Article on the web 31st March 2005***

Kinetic studies involving the use of both stopped-flow and diode array spectrophotometers, show that the reaction between SNAP and captopril in the presence of the metal ion sequestering agent, EDTA, occurs in two well-defined stages. The first stage is a fast reaction while the second stage is slow. The first stage has been postulated to be transnitrosation, and the second stage involves the decay of the newly formed RSNO to effect nitric oxide (NO) release. Both stages are found to be dependent on captopril and $H^+$ concentration. The rates of the transnitrosation increased drastically with increasing pH in the first stage, signifying that the deprotonated form of captopril is the more reactive species. In the case of the second stage the variation in pH showed an increase in rate up to pH 8 after which the rate remained unchanged. Both stages were clearly distinguishable and easily monitored separately. Transnitrosation is a reversible reaction with the tendency for the equilibrium to break down at high thiol concentration. Second-order rate constants were calculated based on the following derived expressions: $-\mathrm{d[SNAP]}/\mathrm{d}t = k_f((K_{\mathrm{SHCapSH}}[\mathrm{CapSH}]_t)/(K_{\mathrm{SHCapSH}} + [\mathrm{H^+}]))[\mathrm{SNAP}]$. $k_f$ is the second-order rate constant for the forward reaction of the reversible transnitrosation process. At 37 °C, $k_f = 785 \pm 14\ \mathrm{M^{-1}\ s^{-1}}$, activation parameters $\Delta H_f^{\ddagger} = 49 \pm 2\ \mathrm{kJ\ mol^{-1}}$, $\Delta S_f^{\ddagger} = -32 \pm 2\ \mathrm{J\ K^{-1}\ mol^{-1}}$. The activation parameters demonstrate the associative nature of the transnitrosation mechanism. The second stage has been found to be very complex, as a variety of nitrogen products form as predicted before. However, the following expression was derived from the initial kinetic data: rate $= k_1K[\mathrm{SNOCap}][\mathrm{CapS^-}]/(K[\mathrm{CapS^-}] + 1)$ to give $k_1 = 13.3 \pm 0.4 \times 10^{-4}\ \mathrm{s^{-1}}$ and $K = 5.59 \pm 0.53 \times 10^4\ \mathrm{M^{-1}}$, at 37 °C, where $k_1$ is the first-order rate constant for the decay of the intermediate formed during the reaction between SNOCap and the remaining excess CapSH present at the end of the first stage reaction. Activation parameters are $\Delta H_1^{\ddagger} = 37 \pm 1\ \mathrm{kJ\ mol^{-1}}$, $\Delta S_1^{\ddagger} = -181 \pm 44\ \mathrm{J\ K^{-1}\ mol^{-1}}$.

## Introduction

Increasing biological and physiological interest has occurred in the field of nitric oxide research owing to its remarkable action *in vivo* as a vasodilator.[1] Not only is focus placed on the molecule itself but also on compounds[2–4] which are able to deliver NO to biological sites. Hence, during the last decade a profound explosion in *S*-nitrosothiol (RSNO) research took place. Focus on *S*-nitrosothiols[1,5,6] is placed more on their ability to store and transport NO in the body owing to the extremely short life of NO which ranges from several minutes *in vitro*,[7] to 1–10 s *in vivo*.[8] Naturally occurring *S*-nitrosothiols such as *S*-nitrosohaemoglobin[9] have shown to be directly linked to blood regulation within the body, and the well-known *S*-nitroso-*N*-acetyl-D,L-penicillamine (SNAP) (Fig. 1) has shown the ability to inhibit platelet aggregation and assist in vasodilation.[10,11] SNAP has already been isolated and its crystal structure obtained.[12] It is a rather stable nitrosothiol, possessing varied values for the half-life ($t_{\frac{1}{2}}$), depending on the concentration of copper(II) and thiolate ion in solution.[5,11,13,14]

Transnitrosation[15,16] is a well-known reaction between RSNOs and thiols and is termed as the transfer of NO from an *S*-nitrosothiol to a thiol to form a new RSNO species [eqn. (1)]. This reaction is of biological importance as the newly formed RSNO may be the better species to effectively deliver NO to cellular components (due to its instability or permeability through cell membranes compared to the original RSNO). But more notable is the fact that this type of reaction is extremely common among RSNOs *in vivo*. In fact, it has been noted that protein activity can be altered due to this process.[17]

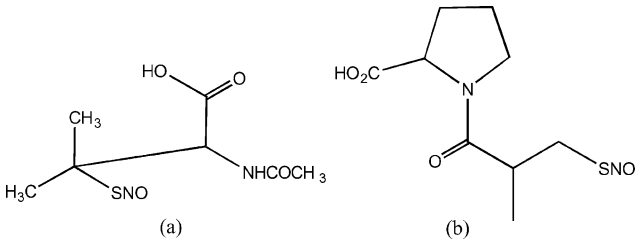


**Fig. 1** Chemical Structures of (a) SNAP, (b) SNOCap.

$$\mathrm{RSNO + RS'H \rightleftharpoons RS'NO + RSH} \quad (1)$$

NO-donating drugs appear to work along with captopril in certain biological reactions,[18] namely, in the inhibition of angiotensin converting enzyme (ACE) activity. The mode by which this occurred, was at the time not very clear. It is therefore the intention of this paper to investigate in detail the underlying possible mechanisms involved in the concomitant addition of the well known NO-donating species, SNAP, to the angiotensin converting enzyme, captopril. This reaction is of particular interest if *S*-nitrosocaptopril (SNOCap) (Fig. 1) is formed from transnitrosation, since the decomposition of the newly formed SNOCap[19,20] would release the biologically significant species, NO and captopril, to the system. Nitric oxide would affect vasodilation, platelet aggregation and its many other functions[21–25] while captopril[26,27] would inhibit angiotensin converting enzyme (ACE), thus establishing the dual activity[28] on the part of SNOCap. It has also been suggested that NO acts

† Electronic supplementary information (ESI) available: Tables of pseudo-first order rate constants for reactions of SNAP with captopril. See http://www.rsc.org/suppdata/ob/b5/b500915d/

DOI: 10.1039/b500915d

 

as an endogenous inhibitor of the ACE and may be additive to the ACE inhibitory effects of captopril.[27]

## Results

### Nature of the reaction

There appears to be an initial rapid reaction between SNAP and captopril, when 0.4 mM SNAP is mixed with 20 mM captopril (CapSH), bringing about a shift in wavelength, as seen in Fig. 2. Each successive spectrum in Fig. 2(a–d) shows a gradual shift from the initial SNAP to the formation of the new nitrosothiol, SNOCap. The wavelength of maximum absorption shifts from 340 nm (indicative of SNAP) to about 332 nm (indicating the presence of SNOCap). Therefore, owing to the closeness of these wavelengths and the resulting overlapping of the spectra, it proved difficult to obtain clear spectral changes, (as shown in Fig. 2) in the UV region. The absorbance-time trace also indicated that this fast reaction could not be monitored in this region. The repetitive scanning was therefore attempted in the visible region of the absorption spectrum, giving rise to the spectra seen in Fig. 3 (a), which clearly shows the rapid simultaneous increase and decrease in absorbance at 547 nm and 590 nm respectively (inset Fig. 3 (a)). This is also observed for the reactions between SNAP and some other well-known thiols.[29] The forbidden $n_N \rightarrow \pi^*$ transition is responsible for the absorption maxima observed in the visible region. The low extinction coefficients of SNAP and SNOCap in the visible region resulted in the necessity to use high concentrations of the reactants to ensure good absorbance changes during the monitoring of the reaction.

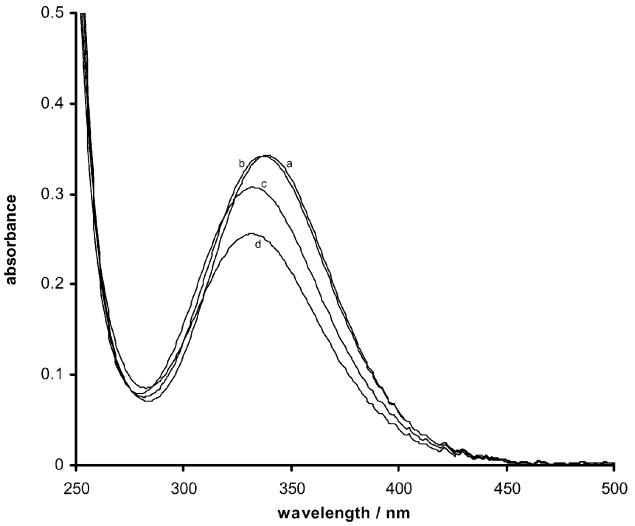


**Fig. 2** Spectral changes during the reaction of SNAP with captopril in the region 250–500 nm. Conditions: 0.4 mM SNAP, 20 mM $[captopril]_T$, pH = 7.0, 50 μM EDTA, ionic strength = 0.5 M (NaCl electrolyte), and at 25 °C. Spectra *a*, *b*, *c* and *d* taken 0.5, 12, 94, and 290 seconds from start of reaction respectively.

After this initial fast reaction, a slow reaction proceeded which could easily be monitored in the UV region of the spectrum as shown in Fig. 3(b). There was a general decrease between *ca.* 300 and 450 nm with a maximum change at 332 nm. The presence of this second stage is also detected in the visible region as the decrease in absorbance at 547 nm, and occurs after rapid increases in absorbance readings at this same wavelength, as shown in Fig. 4. This absorbance–time profile clearly shows the formation and subsequent decay of SNOCap at 547 nm. Owing to the higher extinction coefficients of RSNOs in the UV region, and since there was no interference from other spectra, the second stage was more easily monitored in this region of the spectrum. The final absorbance was *ca.* zero, which strongly confirms the total loss of NO from the RSNO.

### Stoichiometry

Usually, the reaction mixtures are allowed to sit for approximately an hour or more to ensure that the reaction has come to completion, however in this case the absorbances were taken immediately after the solutions were prepared, as it was observed that the solutions rapidly changed colour from green (indicative of the presence of SNAP) to rose-red (indicative of SNOCap) which intensified with time. Hence the rapid formation of SNOCap was clearly indicated by these results as well as the rapid occurrence of transnitrosation. The absorbance readings were again taken after several hours and there was no change in the overall feature of the plot nor the breakpoint previously obtained. Within the range of captopril concentration for stoichiometric studies the overall reaction was found to be 1 : 1 (Fig. 5), and this clearly reflects the first stage of the reaction stoichiometry.

### The variation of captopril concentration

A plot of $k_{obs}$ values *versus* captopril concentration for the first-stage reaction shows a linear dependence on captopril up to a concentration of 0.07 M, as shown by Fig. 6(a). The experimental data are listed in Table 1S.† The plot shows a very small intercept which may relate to the slow self-decomposition of SNAP, or to the presence of an equilibrium process. The second stage is also captopril dependent and a plot of $k_{obs}$ *versus* [captopril] (Table 2S†) results in a straight line with an intercept equal to zero (Fig. 6(b)). This absence of an intercept indicates: (i) the possibility of a large equilibrium constant (of the order $10^3$ and higher) which is known[30] to produce non-measurable intercepts for plots such as that shown in Fig. 6(b), and (ii) the low thermal and photolytic decomposition of SNOCap.

### pH variation

With respect to the first stage; the rates do not increase drastically until about pH 8, where the ionized form of captopril becomes predominant (Table 3S†). Below pH 8, the rates remain slow and slightly unchanged (Fig. 7(a)). In the second stage, rate constants increase to about pH 8 and then remain unchanged beyond pH 8 (Table 4S†), as shown in Fig. 7(b). This stage involves the decomposition of the newly formed SNOCap, in the presence of excess captopril and remaining *N*-acetyl-D,L-penicillamine (products of the first stage). The repetitive scan (Fig. 3(b)) clearly indicates complete decomposition of SNOCap, as it goes to zero absorbance at maximum wavelength of 332 nm. Also, due to the high stability of SNOCap it is safe to deduce that this RSNO species is decomposing by the effect of the thiols present in solution and not due to thermal, photochemical or self-decomposition. The effect of trace metal ions on the decomposition of RSNOs is not a consideration in these reactions, as ethylenediaminetetraacetic acid (EDTA) was added to all reaction mixtures to sequester any trace ions present.

## Discussion

The reaction between SNAP and captopril has yielded two distinct stages. The first stage is transnitrosation while the second-stage is expected to be the decomposition of the newly formed SNOCap. Transnitrosation reactions are known[31,32] to be equilibrium processes. *S*-thiolation[33,34] reactions are slower than transnitrosation reactions and will not affect the kinetics of transnitrosation in this study.

### First stage

The first stage is postulated as transnitrosation and further confirms the accepted view[15,35] that the NO moiety is transferred from SNAP to captopril *via* nucleophilic attack of the thiolate

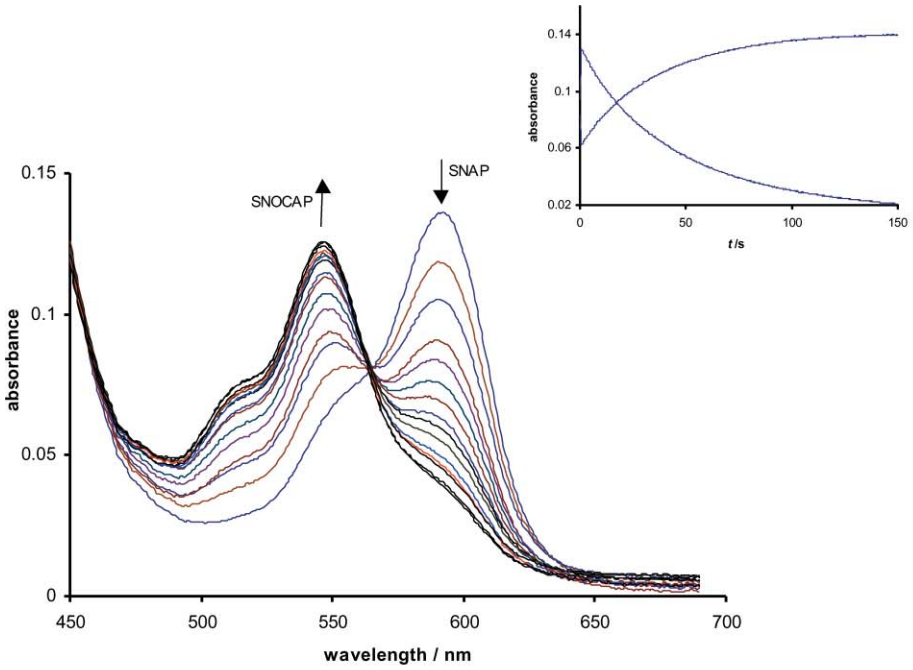


(a)

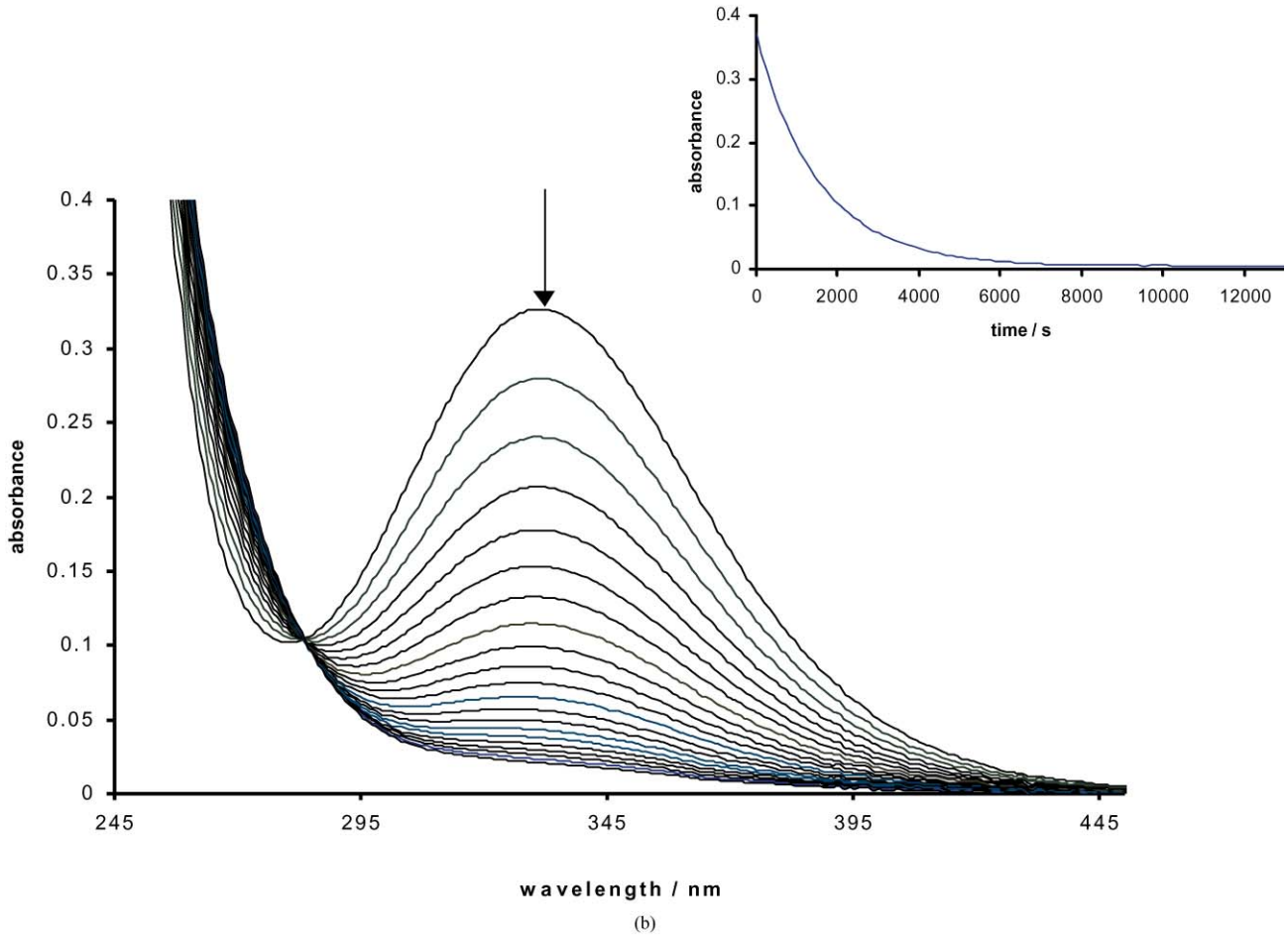


(b)

**Fig. 3** (a) 1st Stage: Spectral changes for the reaction of SNAP with captopril. Conditions: 0.01 M SNAP, 0.03 M $[captopril]_T$, pH = 7.02 (0.1 M phosphate buffer), 50 μM EDTA, ionic strength = 0.5 M (NaCl electrolyte), and at 25 °C. Cycle time of 6 seconds. Inset: Absorbance *versus* time (in seconds). (b) 2nd Stage: Spectral changes for the reaction of SNAP with captopril. Conditions: 0.4 mM SNAP, 20 mM $[captopril]_T$, pH = 7.38 (0.1 M phosphate buffer), 50 μM EDTA, ionic strength = 0.5 M (NaCl electrolyte), and at 25 °C. Cycle time of 4 min. Inset: Absorbance *versus* time (in seconds).

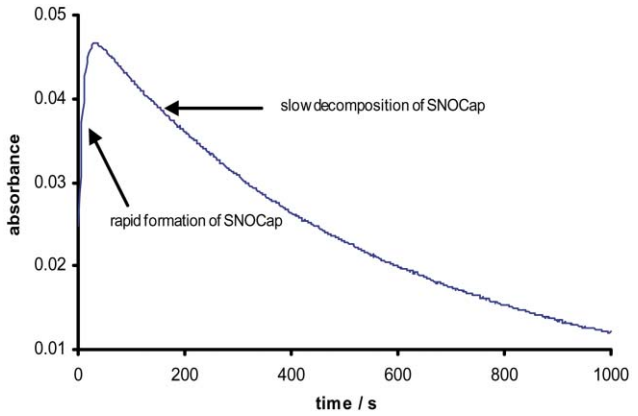


**Fig. 4** Absorbance–time plot for the reaction between SNAP and CapSH at 547 nm. Conditions: 3 mM SNAP, 70 mM $[Captopril]_T$, 50 μM EDTA, pH = 7.30 (0.1 M phosphate buffer), ionic strength = 0.5 M (NaCl electrolyte), at 25 °C.

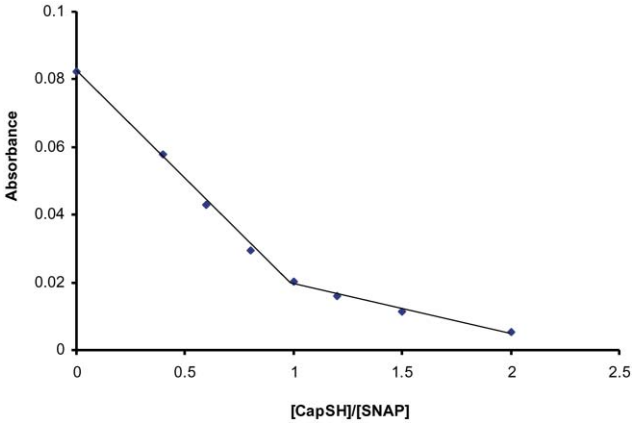


**Fig. 5** Stoichiometric plot for the reaction of SNAP with captopril. Conditions: 0.01 M SNAP, 50 μM EDTA, pH = 6.85 (0.1 M phosphate buffer), ionic strength = 0.5 M (NaCl electrolyte), at 25 °C and $\lambda$ = 590 nm.

anion ($CapS^-$) on the nitrogen atom of NO in SNAP, to yield *S*-nitrosocaptopril (SNOCap). At higher pHs, the deprotonated form of captopril ($pK_{CapSH}$ 9.8)[36] is the predominant species, as such the thiolate anion ($CapS^-$) is the driving force of the reaction and is indicated by the increase in rates with increase in pH. Hence, the reactions indicated by $k'_f$, $k'_r$ and $k_r$ in Scheme 1 are not included in the rate expression.

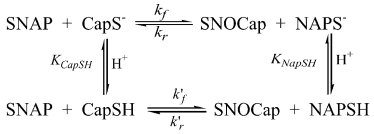


**Scheme 1** Reaction mechanism for the first stage of the reaction between SNAP and CapSH.

Excess captopril will drive the equilibrium to the right, thus limiting the occurrence of the reverse reaction ($k_r$). This is actually the case, as values for $k_r$ have errors as high as 300%, and as such these values are not reported in this study. Hence,

$$\text{Rate} = \frac{-\text{d[SNAP]}}{\text{d}t} = k_f[\text{CapS}^-][\text{SNAP}]$$

(assuming $k_r$ is negligible) (2)

The value of $[CapS^-]$ can be derived from the equilibrium equation in Scheme 1 as,

$$[\text{CapS}^-] = \frac{K_{\text{CapSH}}[\text{CapSH}]_T}{[\text{H}^+] + K_{\text{CapSH}}}, \quad (3)$$

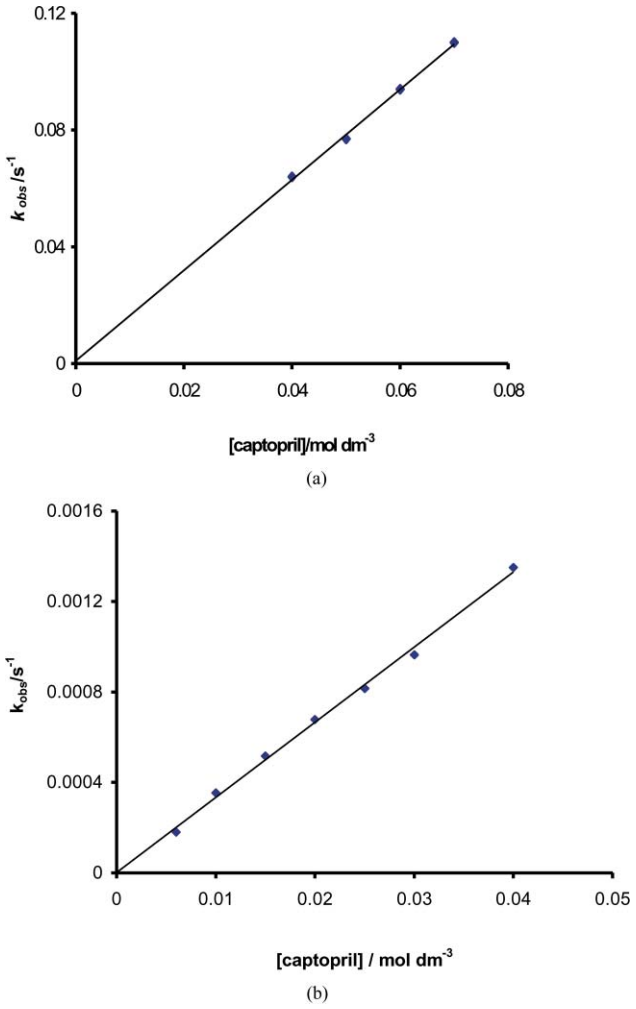


**Fig. 6** (a). 1st Stage : Captopril-dependent decomposition of SNAP. Conditions: 3 mM [SNAP], 40–70 mM $[CapSH]_T$, 50 μM [EDTA], ionic strength = 0.5 M (NaCl electrolyte), temp = 25 °C, pH = 7.30 (0.1 M phosphate buffer), $\lambda$ = 590 nm. (b). 2nd Stage: Captopril-dependent decomposition of SNAP. Conditions: 0.4 mM [SNAP], 6–40 mM $[CapSH]_T$, 50 μM [EDTA], ionic strength = 0.5 M (NaCl electrolyte), temp = 25 °C, pH = 7.38 (0.1 M phosphate buffer), $\lambda$ = 332 nm.

$[CapSH]_T$ is the total captopril concentration employed in the reactions. Substituting the value of $[CapS^-]$ into eqn. (2), the rate expression for the reaction is obtained.

$$\text{Rate} = k_f \frac{K_{\text{CapSH}}[\text{CapSH}]_T}{[\text{H}^+] + K_{\text{CapSH}}}[\text{SNAP}] \quad (4)$$

Under pseudo-first-order condition,

$$k_{obs} = k_f \frac{K_{\text{CapSH}}[\text{CapSH}]_T}{[\text{H}^+] + K_{\text{CapSH}}} \quad (5)$$

Using eqn. (5), the non-linear regressional analysis of the experimental data in Table 3S was carried out utilising the computer programme (Sigma Plot-Jandel Scientific, USA). Values of the calculated pseudo-first-order rate constants obtained from the analysis are also listed in Table 3S. It should be noted that the error associated with the $k_{obs}$ values at high $[H^+]$, *i.e.* low pH values (pH 6.3 and 6.7), are high, since the concentration of $CapS^-$ is negligible at these pH values. The fitted curve generated from the analysis is shown in Fig. 7(a). The values of $k_f$ as listed in Table 1 are associated with a very small error (~2%) at the temperatures indicated. The quantification of $[NAPSH]_T$ was done as outlined by Wang *et al.*[31]

The comparatively low activation enthalpy ($\Delta H_f^{\ddagger}$ = 49 ± 2 kJ $mol^{-1}$), combined with a negative entropy of activation ($\Delta S_f^{\ddagger}$ = −32 ± 2 J $K^{-1}$ $mol^{-1}$) indicates a facile nucleophilic

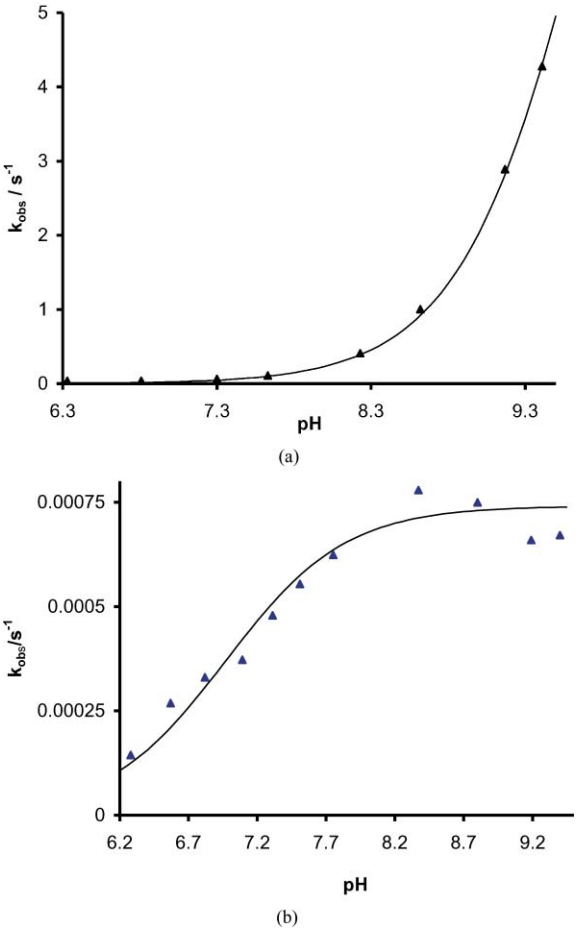


**Fig. 7** (a). 1st Stage: Observed first-order rates ($k_{obs}$) *versus* pH for the reaction between SNAP and Captopril. Conditions : 3 mM [SNAP], 40 mM $[CapSH]_T$, 50 μM [EDTA], ionic strength = 0.5 M (NaCl), $\lambda$ = 590 nm, and at 25 °C. (▲) Experimental points and (—) calculated line from eqn. (5). (b). 2nd Stage: Observed first-order rates ($k_{obs}$) *versus* pH for the reaction between SNAP and Captopril. Conditions : 0.4 mM [SNAP], 15 mM $[CapSH]_T$, 50 μM [EDTA], ionic strength = 0.5 M (NaCl), λ = 332 nm, and at 25 °C. (▲) Experimental points and (—) calculated line from eqn. (8).

attack by captopril *via* an ordered transition state as described below.

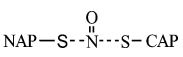


### Second stage

Since there is some change in the rate constant in the pH range 6.5 to 8, it can be assumed that the ionized form of captopril ($CapS^-$) is participating in this second stage reaction as well. It is important to note that within this same pH range, the fully protonated form of captopril has its concentration unchanged. The very high stability of SNOCap (formed at the end of the first stage), indicates the possible formation of an intermediate (**I**) to facilitate its breakdown. An unstable three member ring intermediate (Scheme 2) has been proposed; which readily breaks apart to give the disulfide and $NO^-$ due to the delocalized electrons on the nitrogen of nitric oxide. It is quite apparent from the data in Table 4S that only the deprotonated form of captopril is the reactive species which forms the intermediate, since a clear indication of saturation is observed in the pH variation data, and on the basis of this observation, a mechanism depicted in Scheme 2 is proposed.

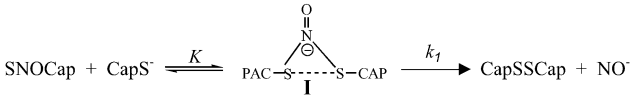


**Scheme 2** Mechanism for the 2nd Stage reaction.

The rate expression deduced from the above mechanism is shown as eqn. (6).

$$\text{Rate} = \frac{k_1 K[\text{CapS}^-][\text{SNOCap}]}{K[\text{CapS}^-] + 1} \quad (6)$$

Under pseudo-first-order condition with respect to captopril, eqn. (6) becomes eqn. (7).

$$k_{obs} = \frac{k_1 K}{K + 1/[\text{CapS}^-]} \quad (7)$$

On substituting the value of $[CapS^-]$ from eqn. (3) into eqn. (7), the calculated pseudo-first-order rate constant becomes:

$$k_{obs} = \frac{k_1 K}{\left(\frac{[H^+]+K_{CapSH}}{K_{CapSH}[CapSH]_T}\right) + K} \quad (8)$$

$K$ and $k_1$ are the equilibrium and first-order rate constants respectively for the overall reaction in Scheme 2, and are obtained from the incorporation of eqn. (8) into the Sigma Plot program. Although eqn. (8) appears to be non-linear with respect to $[CapSH]_T$, the first-order dependency of the captopril is justified because the other parameters in the denominator of the rearranged equation are negligible with respect to $[H^+]$.

The calculated $k_{obs}$ are shown as the solid line in Fig. 7(b), while the experimental values are indicated by the data points. Beyond pH 8.2 there is scattering, but the rate constants appear to be relatively unchanged within experimental errors. Second-order rate constants are derived from the product of $K$ and $k_1$ and are shown in Table 1.

The intermediate with a three member ring structure has been proposed on the basis of a facile production of disulfide[37,38] and $NO^-$. Both species have been reported as possible products in other nitrosation reactions. Singh *et al.*[39] reported production of ammonia and nitrous oxide, with nitrous oxide presumably produced almost quantitatively from $NO^-$, from the transnitrosation reaction between glutathione molecules. In our case, nitrous oxide has also been detected as one of the byproducts. The large equilibrium constant ($K$) values indicate a strong

**Table 1** Second-order rate constants and activation parameters for the reductive decomposition of SNAP by captopril[a]

| $T$/°C | $k_f/10^2$ dm$^3$ mol$^{-1}$ s$^{-1}$ | $k_1/10^{-4}$ s$^{-1}$ | $K/10^4$ dm$^3$ mol$^{-1}$ | $k_2$/dm$^3$ mol$^{-1}$ s$^{-1}$ |
|---|---|---|---|---|
| 20.2 | 2.57 ± 0.04 | 5.48 ± 0.16 | 3.61 ± 0.21 | 19.8 ± 1.3 |
| 25.2 | 3.75 ± 0.03 | 7.42 ± 0.22 | 4.50 ± 0.30 | 33.4 ± 2.4 |
| 30.2 | 5.41 ± 0.08 | 9.57 ± 0.30 | 5.66 ± 0.40 | 54.2 ± 4.2 |
| 37.0 | 7.98 ± 0.14 | 13.3 ± 0.40 | 5.59 ± 0.53 | 74.4 ± 7.4 |
| | $\Delta H_f^{\ddagger}$/kJ mol$^{-1}$ | $\Delta H_1^{\ddagger}$/kJ mol$^{-1}$ | | |
| | 49 ± 2 | 37 ± 1 | | |
| | $\Delta S_f^{\ddagger}$/J K$^{-1}$ mol$^{-1}$ | $\Delta S_1^{\ddagger}$/J K$^{-1}$ mol$^{-1}$ | | |
| | −32 ± 2 | −181 ± 44 | | |

[a] $k_f$ is derived from eqn. (5). $k_1$ and $K$ are derived from eqn. (8). $k_2 = k_1 \times K$.

driving force towards the formation of an intermediate which releases nitroxyl ion in a rate determining process.

It is interesting to note that the activation enthalpy ($\Delta H_1^{\ddagger} = 37 \pm 1$ kJ mol$^{-1}$) for this second stage is smaller than that of the first stage, although the reaction is much slower than that of the first stage reaction. This is because the $\Delta H_1^{\ddagger}$ has been compensated by the large entropy of activation ($\Delta S_1^{\ddagger} -181 \pm 44$ J K$^{-1}$ mol$^{-1}$). The large and negative entropy of activation is justified due to the expected formation of a well organized transition state where S–N bond breaking occurs to form the stable disulfide.

In the presence of various reductants it is not surprising that the reduced form of $^{\bullet}$NO, the nitroxyl ion, $NO^-$, is the nitrogen product of the second stage reaction. It has been established[40] that the interconversion of $NO^-$, $^{\bullet}NO$ and $NO^+$ can take place under cellular conditions, so all three species should be considered when establishing the biological activity of nitric oxide. Under the experimental conditions employed, a number of subsequent complex reactions (not shown) are possible which may lead to the formation of a variety of nitrogen containing species.[41] Wong *et al.*[41] proposed a comprehensive reaction scheme which accounts for all the *N*-species identified at the end of such reactions involving a thiol and an *S*-nitrosothiol. This proposed scheme speaks to the complexity of such RSNO–R*SH reactions and the variety of routes that can lead to the decomposition of RSNO in the presence of R*SH. The more commonly met *N*-products detected under aerobic conditions using [SNAP] = 0.2 mM, $[CapSH]_T$ = 2 mM, pH = 7.2, $I$ = 0.5 M (NaCl) and at 25 °C; were $NO_2^-$ = 37%, NO ≤ 5% and $NH_2OH$ = 1%. These results are based upon the initial [SNAP] and are averages of duplicate determinations. Any unaccounted percentage could be of $NH_3$, and $N_2O$. $N_2O$ was also detected (but not quantified) by GC-MS.

## Experimental

### Materials

SNAP was prepared and its purity checked according to previous experiments.[12] The NO vibration frequency obtained from infra-red analysis was 1480 cm$^{-1}$ (Lit.[13] 1483 cm$^{-1}$). The product was obtained in a 70% yield with a melting point of 152–154 °C, (Lit.,[12] 68% yield and mp 152–154 °C). The maximum wavelengths ($\lambda_{max}$) and corresponding extinction coefficients ($\varepsilon$) obtained were 340, 590 nm ($H_2O$); and 1042, 13 M$^{-1}$ cm$^{-1}$, respectively (Lit.[6] ($H_2O$) 340, 590 nm; 815, 12 M$^{-1}$ cm$^{-1}$).

Captopril was obtained from Sigma Chemical Company, and was of analytical grade, obtained in at least 99% purity.

All other chemicals were also obtained from either Sigma or Aldrich Chemical companies, and of the same grade and purity. All reactions were carried out in deionized water, obtained from a Labconco Water Processor. EDTA was added to all experiments so as to eliminate catalysis by trace quantities of metal ions, namely copper.

### Stoichiometric determination

A series of molar ratios of captopril and SNAP were mixed together under an inert (argon) atmosphere. The final absorbance values were then measured at 590 nm (wavelength of maximum absorption change for SNAP) and plotted against the [total captopril]/[SNAP] ratio in order to determine the reaction stoichiometry, which would be indicated by the distinct breakpoint in the graphical plot.

### Kinetic measurements

The first stage of the reaction was monitored on a Hi-Tech Scientific SF61 DX2 stoppped-flow system (with a diode array rapid scanning option) interfaced with a DELL V333c computer and operated by a KinetAsyst software (ver. 2.2, 1999). The second stage was monitored on a Hewlett-Packard 8453 Diode Array instrument, equipped with a multicell transport system and interfaced with a ChemStation programme. All kinetic measurements were thermostatted at the required temperature by a PolyScience Digital Temperature Controller with the use of a circulating bath. The first stage of the reaction was monitored at both 590 (SNAP decay) and 547 nm (SNOCap formation) and not in the ultra-violet region of the spectrum, as there was a close overlap of the peaks belonging to SNAP (340 nm) and SNOCap (332 nm). The reaction between SNAP and CapSH was studied under aerobic conditions, and the following parameters were employed for a detailed kinetic study.

**First stage.** Studies were done over the range 0.04 ≤ [captopril] ≤ 0.07 mol dm$^{-3}$, 6.3 ≤ pH ≤ 9.4, 20 ≤ temperature ≤ 37 °C, [SNAP] = 3 mM, [EDTA] = 50 μM, and at fixed ionic strength of 0.5 M (NaCl). Analyzing data at both wavelengths (*i.e.* 547 nm and 590 nm) gave the same results, and only those at 590 nm are reported. Very good first-order behaviour was observed and pseudo-first-order rate constants ($k_{obs}$) reported are the average of two kinetic runs with less than 5% standard deviation. Ionic strength ($I$) was maintained at 0.5 M, using NaCl as the supporting electrolyte.

**Second stage.** This stage was studied at 332 nm, with [SNAP] = 0.4 mM, [EDTA] = 50 μM, and over the ranges 0.006 ≤ [captopril] ≤ 0.04 mol dm$^{-3}$, 6.3 ≤ pH ≤ 9.4, 20 ≤ temperature ≤ 37 °C, and at fixed ionic strength of 0.5 M (NaCl).

### pH Studies

pHs below 8 were maintained using phosphate buffer while borate buffer was used to maintain pHs above 8. Prior to use, stock solutions of captopril were taken to near neutral with NaOH. The actual pHs of the reaction mixtures were analyzed using an Orion Expandable Ion Analyzer EA 920 meter fitted with Cole Parmer electrodes.

### Product detection

**Nitric oxide.** A calibrated World Precision ISO-NOP electrode fitted to a WPI ISO-NO Mark II meter was employed in detecting NO in the reaction systems (saturated with argon gas). Calibration of the electrode was done by generating NO from the reaction of $NaNO_2$ with excess $H_2SO_4$ and KI. A continuous flow of argon was maintained at approximately 250 cm$^3$ min$^{-1}$ and vessel pressure about 1 atm.

**Nitrite.** The oxidation of nitric oxide is expected to give nitrite under aerobic conditions, and is easily detected *via* the spectrophotometric method known as the Griess test.[42] This test is based on a diazotisation reaction whereby the resulting intensity of the red coloured complex is directly proportional to nitrite concentration, and is measured photometrically. The experimental samples (at pH 7) were treated in the same manner as the standards and checked against the calibration curve in order to calculate the concentration of nitrite in the solution.

**Hydroxylamine.** The presence of hydroxylamine ($NH_2OH$) was detected according to Magee and Burris,[43] by noting the absorbances of the test solutions at 705 nm on a conventional UV-VIS spectrophotometer.

**Nitrous oxide.** Nitrous oxide[44] was identified by GC-mass spectrometry, as the headspace gas of selected experiments under anaerobic conditions. This method is not suitable for the quantification of nitrous oxide ($N_2O$).

## Acknowledgements

The authors wish to thank the Department of Chemistry and the Board of Graduate Studies at the University of the West Indies, Mona for funding this project.

## References


1 A. R. Butler and P. Rhodes, *Anal. Biochem.*, 1997, **249**, 1–9.
2 P. G. Wang, M. Xian, X. Tang, X. Wu, Z. Wen, T. Cai and A. Janczuk, *Chem. Rev.*, 2002, **102**, 1091–1134.
3 D. L. H. Williams, *Adv. Phys. Org. Chem.*, 1983, **19**, 381–429.
4 E. Iglesias and J. Casado, *Int. Rev. Phys. Chem.*, 2002, **21**, 37–74.
5 D. L. H. Williams, *Acc. Chem. Res.*, 1999, **32**, 869–876.
6 K. Szaciłowski and Z. Stasicka, *Prog. React. Kinet. Mech.*, 2000, **26**, 1–58.
7 J. S. Beckman and W. H. Koppenol, *Am. J. Physiol.*, 1996, **271**, C1424–C1437.
8 L. J. Ignarro, J. M. Fukuto, J. M. Griscavage, N. E. Rogers and R. E. Burns, *Proc. Natl. Acad. Sci. USA*, 1993, **90**, 8103–8107.
9 L. Jia, C. Bonaventura, J. Bonaventura and J. S. Stamler, *Nature*, 1996, **380**, 221–226.
10 E. Salas, M. A. Moro, S. Askew, H. F. Hodson, A. R. Butler, M. W. Radomski and S. Moncada, *Br. J. Pharmacol.*, 1994, **112**, 1071–1076.
11 S. C. Askew, A. R. Butler, F. W. Flitney, G. D. Kemp and I. L. Megson, *Bioorg. Med. Chem.*, 1995, **3**, 1–9.
12 L. Field, R. V. Dilts, R. Ravichandran, P. G. Lenhert and G. E. Carnahan, *J. Chem. Soc., Chem. Commun.*, 1978, 249–250.
13 B. Roy, A.-M. d'Hardemere and M. Fontecave, *J. Org. Chem.*, 1994, **59**, 7019–7026.
14 A. P. Dicks, P. H. Beloso and D. L. H. Williams, *J. Chem. Soc., Perkin Trans. 2*, 1997, 1429–1434.
15 D. J. Barnett, J. McAninly and D. L. H. Williams, *J. Chem. Soc., Perkin Trans. 2*, 1994, 1131–1133.
16 Z. Liu, M. A. Rudd, J. E. Freedman and J. Loscalzo, *J. Pharmacol. Exp. Ther.*, 1998, **284**, 526–534.
17 N. Hogg, *Free Rad. Biol. Med*, 2000, **28**, 1478–1486.
18 K. Persson, P. A. Whiss, K. Nyhlen, M. Jacobsson-Strier, M. Glindell and R. G. G. Andersson, *Eur. J. Pharmacol.*, 2000, **406**, 15–23.
19 J. Loscalzo, D. Smick, N. Andon and J. Cooke, *J. Pharm. Exp. Ther.*, 1989, **249**, 726–729.
20 J. Cooke, N. Andon and J. Loscalzo, *J. Pharm. Exp. Ther.*, 1989, **249**, 730–734.
21 A. R. Butler and D. L. H. Williams, *Chem. Soc. Rev.*, 1993, **22**, 233–241.
22 J. F. Kerwin, Jr., J. R. Lancaster, Jr. and P. L. Feldman, *J. Med. Chem.*, 1995, **38**, 4343–4362.
23 P. L. Feldman, O. W. Griffith and D. J. Stuehr, *Chem. Eng. News*, December 20, 1993, 26–37.
24 M. W. Radomski, R. M. J. Palmer and S. Moncada, *Lancet*, 1987, **2**, 1057–1058.
25 M. W. Radomski, R. M. S. Palmer and S. Moncada, *Proc. Natl. Acad. Sci. USA*, 1990, **87**, 5193–5197.
26 E. Kalkman, P. van Haren, P. R. Saxena and R. G. Schoemaker, *Eur. J. Pharmacol.*, 1999, **369**, 339–348.
27 K. Persson and R. Andersson, *Eur. J. Pharmacol.*, 1999, **385**, 21–27.
28 J.-W. Park, *Biochem. Biophys. Res. Commun.*, 1992, **189**(1), 206–210.
29 D. Aquart, PhD Thesis, University of the West Indies, 2002.
30 P. H. Beloso and D. L. H. Williams, *Chem. Commun.*, 1997, 89–90.
31 K. Wang, Z. Wen, W. Zhang, M. Xian, J.-P. Cheng and P. G. Wang, *Bioorg. Med. Chem. Lett.*, 2001, **11**, 433–436.
32 N. Hogg, *Anal. Biochem*, 1999, **272**, 257–262.
33 C. M. Padgett and A. R. Whorton, *Arch. Biochem. Biophys.*, 1998, **358**, 232–242.
34 N. Hogg, R. J. Singh and B. Kalyanaraman, *FEBS Lett.*, 1996, **382**, 223–228.
35 D. J. Barnett, A. M. Rios and D. L. H. Williams, *J. Chem. Soc., Perkin Trans. 2*, 1995, 1279–1282.
36 *The Merck Index-An Encyclopedia of Chemicals, Drugs and Biologicals*, Merck & Co., Inc., Rahway, NJ, USA, 1983.
37 J.-W. Park, *Biochem. Biophys Res. Commun.*, 1988, **152**, 916–920.
38 D. J. Meyer, H. Kramer, N. Ozer, B. Coles and B. Ketterer, *FEBS Lett.*, 1994, **345**, 177–180.
39 S. P. Singh, J. S. Wishnok, M. Keshive, W. M. Deen and S. R. Tannenbaum, *Proc. Natl. Acad. Sci. USA*, 1996, **93**, 14428–14433.
40 M. N. Hughes, *Biochim. Biophys. Acta*, 1999, **1411**, 263–272.
41 P. S.-Y. Wong, J. Hyun, J. M. Fukuto, F. N. Shirota, E. G. DeMaster, D. W. Shoeman and H. T. Nagasawa, *Biochemistry*, 1998, **37**, 5362–5371.
42 G. H. Jeffery, J. Bassett, J. Mendham and R. C. Denney, *Vogel's Textbook of Quantitative Chemical Analysis*, 5th Ed., Longman Group, UK, 1989, p. 702.
43 W. E. Magee and R. H. Burris, *Am. J. Bot.*, 1954, **41**, 777–782.
44 J. N. Smith and T. P. Dasgupta, *J. Inorg. Biochem.*, 2001, **87**, 165–173.